Desorption influence of water on structural, electrical properties and molecular order of vanadium pentoxide xerogel films

C.L. Londoño-Calderón, C. Vargas-Hernández, and J.F. Jurado
Laboratorio de Propiedades Ópticas de Materiales,
Departamento de Física y Química, Universidad Nacional de Colombia,
A.A 127, Manizales, Colombia,
e-mail: jfjurado@unal.edu.co

Recibido el 16 de junio de 2010; aceptado el 18 de agosto de 2010

Vanadium pentoxide xerogel films were grown by sol-gel method on pre-treated glass substrates, the gelation time was 14 days. The crystallinity of the films was analyzed with X-ray diffraction (XRD), identifying the composite $V_2O_5{\cdot}nH_2O$ before, and both vanadium pentoxide xerogel and α-V_2O_5 phases after, being subjected to thermal treatment (47, 97, 147, 204, 237, 272, 297 and 330°C during 15 minutes in each isotherm). The termal treatment reduces the degree of hydrations gel (n) from 2.1 to 1.4, besides the secondary phase (α-V_2O_5) has lattice parameters very similar to the precursor powder (which deviate about 0.3%). The electrical conductivity presents a semiconductor behavior in agreement with small polaron model, thermally activated and irreversible. The activation energies for three consecutive cycles were studied and analyzed: a strong dependency between the degree of hidratation's gel n with activation energy for high and low temperature regions was found. μ-Raman Spectroscopy showed the influence of temperature in the vanadium pentoxide gel film, presenting a phase transition from crystalline-amorphous for temperatures above 272°C and inferring that the water presence in the sample is responsible in some way for the crystallinity of the material.

Keywords: V_2O_5 xerogel; XRD; electrical conductivity; μ-Raman.

Películas del xerogel pentóxido de vanadio, fueron crecidas por el método de sol gel sobre substratos de vidrio previamente tratados, el tiempo de gelación fue de 14 días. La cristalinidad de las películas fue analizada con difracción de rayos-X (XRD), identificando el composito $V_2O_5{\cdot}nH_2O$ antes y las fases pentóxido de vanadio xerogel y α-V_2O_5, después de ser sometidas a tratamiento térmico (47, 97, 147, 204, 237, 272, 297 y 330°C durante 15 minutos en cada isoterma). El tratamiento térmico reduce el grado de hidratación del gel (n) desde 2.1 hasta 1.4. La fase secundaria (α- V_2O_5) tiene parámetros de red muy similares a los del precursor en polvo (los cuales no sobrepasan el 0.3%). La conductividad eléctrica presenta un comportamiento tipo-semiconductor de acuerdo con el modelo del pequeño polarón, térmicamente activado e irreversible. Las energías de activación para tres ciclos consecutivos fueron estudiados y analizados, encontrándose una fuerte dependencia entre el grado de hidratación del gel n con la energía de activación, para las regiones de altas y bajas temperaturas. Espectroscopía μ-Raman mostró la influencia de la temperatura sobre las películas del gel óxido de vanadio, presentando una transición de fase de cristalino-amorfo para temperaturas superiores 272°C, infiriendo que la presencia del agua en la muestra es responsable de alguna forma de la cristalinidad del material.

Descriptores: Pentóxido de vanadio; XRD; conductividad eléctrica; micro-Raman.

PACS: 81.20.Fw; 61.05.cp; 73.61.-r

1. Introduction

The V_2O_5 has an orthorhombic, laminar type structure, composed by squared pyramids of oxygen and vanadium atoms on its bases, generating a high anisotropy that makes possible the ions and polymeric molecules insertion over the matrix material [1,2], forming stable phases with interesting properties in the technological level.

The hydrated vanadium pentoxide $V_2O_5 \cdot nH_2O$ has been widely studied [3]; however, the exact nature and its structural ordering is not even totally clear. The hydrated vanadium oxides are often described as nano-composites materials, they are made by a liquid phase (water molecules) trapped in a lattice oxide. Strong interactions occur in order that oxide-water interface and the vanadium oxide gel behave like a monophasic system [4]. Because of this, the electrical properties, are dominated by the electrons hopping between mixed valence vanadium (V^{4+} and V^{5+}), while on the other hand, an ion conduction component arises due to the protons diffusion in the aqueous phase that in large extent are correlated to the method and growth technique. Many discrepancies are found in the literature about the electrical conductivity of vanadium oxide films at room temperature, showing a strong dependency of many parameters, such as: the reduced quantity ions V^{4+}, the atmospheric relative humidity, the gel hydration state (n), the aging and even the film thickness [3].

Most of the films obtained from these gels present crystallographic orientations, corresponding to the (001), (003), (004) and (005) planes [5], where the H_2O insertion over matrix material is along the *c* crystallographic direction modifying the interplanar distances between basal planes.

The purpose if this work is to determine the water molecules desorption influence over the structural, electrical and molecular properties of $V_2O_5{\cdot}nH_2O$ ($n{\approx}2.1$) over glass, synthesized by the peroxovanadic acid route for 14 days gelation time by slow immersion on the solution.

TABLE I. Lattice parameter for the growth film ($V_2O_5 \cdot nH_2O$), before* and after** thermal treatment.

LP[a]	Numeric value* (Å)	Numeric value** (Å)
c	12.480	10.620
Δc	0.130	0.006

[a] Lattice parameter

TABLE II. Crystallite size for the growth film ($V_2O_5 \cdot nH_2O$), before* and after** thermal treatment.

CP[a]	SC*[b] (Å)	SC** (Å)
001	52.405	107.273
003	31.645	50.915
004	58.640	–
005	84.231	–

[a] Crystallographic planes. [b] Crystallite size

TABLE III. Lattice parameters for the pure vanadium pentoxide and film growth (secondary phase), after thermal treatment.

LP[a]	Pure (Å)	Secondary phase (Å)
a	11.514	11.523
b	3.566	–
c	4.369	4.381

[a] Lattice parameters.

TABLE IV. Crystallite size for the film growth (secondary phase) and pure vanadium pentoxide.

CP[a]	Secondary phase (Å)	Pure (Å)
001	643.906	2009.070
101	563.133	1210.975
002	750.291	1170.782
302	331.350	511.667

[a] Crystallographic planes

TABLE V. Activation energies from pure vanadium pentoxide.

Region	E_a(eV)[a]	$\pm \Delta E_a$(eV)
High temperature	0.361	0.002
Low temperature	0.231	0.001

[a] Activation energies.

TABLE VI. Activation energies from vanadium pentoxide xerogel growth film for different cycles.

Cycle Number	E_a(eV)[a]	E_a(eV)[b]
1	0.295	0.265
2	0.328	0.276
3	0.377	0.292

[a] High temperature region. [b] Low temperature region.

2. Experimental details

We mixed V_2O_5 Acros Organics mark with $99,6\%$ purity, with hydrogen peroxide (H_2O_2) aqueous to the 10%. The hydrogen peroxide decomposition takes place while O_2 is released. The solution begins with an orange coloration during the first minutes and then becomes a dark red after few hours. As time goes by the bubbling slows, stopping progressively. The obtained solution was left immobile during 14 days, time for which the solution had become quite viscous and was magnetically stirred during 3 hours. Glass substrates previously treated and cleaned by means of ultrasound were slowly immersed in the solution obtaining a thick layer (about of 15 ± 5 μm), which were left to dry in room conditions during 24 hours.

Crystal structure of the material at room temperature was determined for the film before and after being subjected to 47, 97, 147, 204, 237, 272, 297 and $330°$C thermal treatment during 15 minutes in each isothermal with an A8 Advance Buker AXS equipment, Cu-Kα, monochromatic radiation source in a range between $5° \leq 2\theta \leq 50°$.

The electrical conductivity, as a function of temperature, was measured by using the four-probe conventional Van der Pauw method, in the temperature range between 346-505 K and pressure of one atmosphere for fresh films between consecutive cycles.

The molecular ordering was studied as a function of temperature in-situ for a fresh sample, using a LabRam HR800 equipment of the Horiba Jobin Yvon make of high resolution, monochromatic radiation source of 473 nm, 5,5 mW power, 2 mm of area exhibition in the 100-1200 cm^{-1} spectral range. The sample was warmed up and stabilized during 15 minutes in each isothermal.

3. Results and discussion

3.1. X-Ray diffraction analysis

Figure 1 shows the diffractograms for the fresh $V_2O_5 \cdot nH_2O$ films (14 gelation days) before and after being subjected to the thermal treatment. The spectrum fresh film (Fig. 1a) presents a preferential growth for (001) plane accompanied by (003), (004) and (005) crystallites, which is in agreement with the reported for these kind of films [5]. After being subjected to the thermal treatment, it presents two phases' types which correspond to $V_2O_5 \cdot nH_2O$ (for 001 and 003 peaks) and α-V_2O_5 [6] (see Fig. 2) for 001^*, 101^*, 002^* and 302^*.

The lattice parameter c for the fresh film growth

$$(V_2O_5 \cdot nH_2O)$$

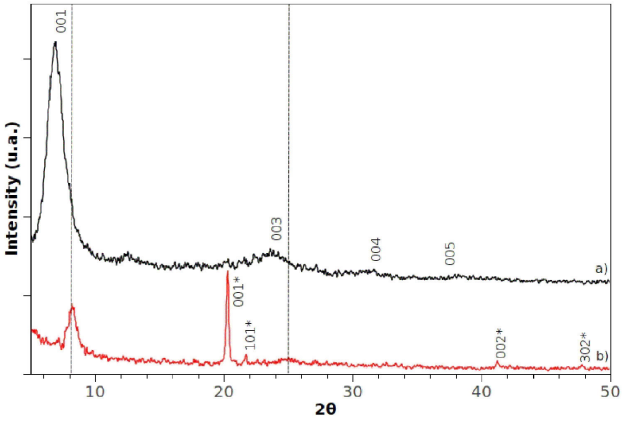

FIGURE 1. X-Ray diffraction pattern at room temperature of V_2O_5 xerogel, before (a) and after (b) thermal treatment for α-V_2O_5.

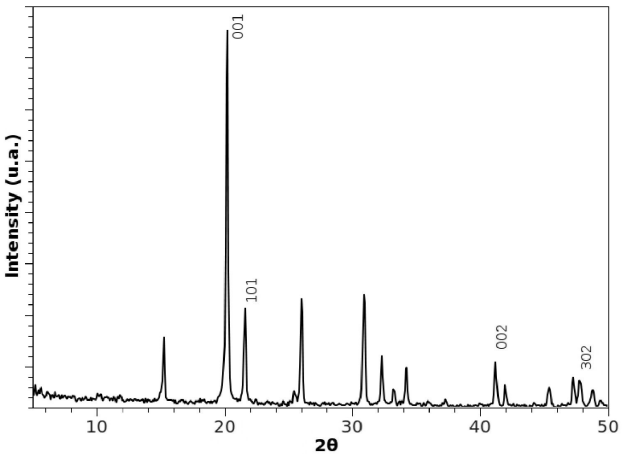

FIGURE 2. X-Ray diffraction pattern at room temperature of V_2O_5 precursor in powder.

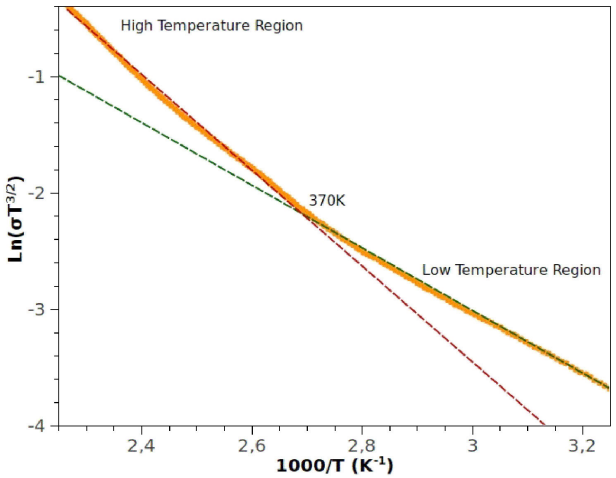

FIGURE 3. Electrical conductivity vs. temperature function from V_2O_5 sprinkle film. The dashed lines represent best fits .

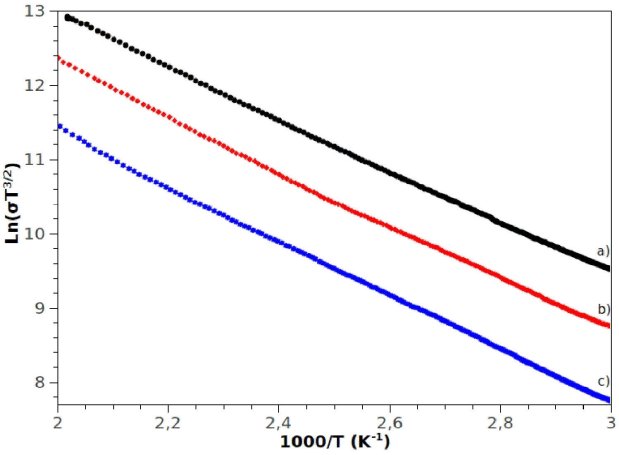

FIGURE 4. Electrical conductivity vs. temperature function from V_2O_5 xerogel fresh film for; a) first, b) second and c) third consecutive cycles.

decreases with the thermal treatment (see Table I) due to a gel hydration reduction; while the crystallite size for each peak of the diffractogram increases (see Table II). The Cohen method and the Scherrer formula were used [7], with the respectively correction of the instrumental FWHM; besides, the crystallite sizes average (5.7 nm) are in agreement with recent reports [8]. The interplanar distance d_{001} value found for the film before the thermal treatment (12.8 Å) is valid for n≈2.1 [9]; and after thermal treatment $d_{001} = 10.8$ Å, with n≈1.4 using the Van der Waals diameter for the water molecule (2.7 Å) [3].

The lattice parameters for the V_2O_5, for the secondary phase and V_2O_5 powder precursor are shown in Table III, the differences don't overcome 0.3%. The film treated thermally does not crystallize in the *b* crystallographic direction; maybe due to a strong linkage of water molecules in that direction. The crystallite size (see Table IV) for the film growth(vanadium pentoxide secondary phase) and pure powder V_2O_5, are in a value average of 572 and 1226 Å respectively.

3.2. Electrical characterization

Figure 3 shows the electrical conductivity as a function of temperature for V_2O_5 powder percursor, evidencing a semiconductor behavior in agreement with the small polaron model [10]. In the figure, two regions with different activation energies (E_a) were differentiated (see Table V), which are explained by the presence of bound polarons trapped on vanadium sites associated with oxygen vacancies (low temperature region) and free polarons hopping between the other vanadium sites (high temperature region). A comparison between the activation energies observed above and below 370 K, could give a rough estimate of the needed energy for ionization of localized defects. It is $E \approx 0.13$ eV, a value in agreement with previous reports [10].

From $V_2O_5{\cdot}nH_2O$ film growth (see Fig. 4), the electrical conductivity presents two contributions: ionic and electronic. The first constituted by the aqueous phase, while the second by mixed valence vanadium ions. It would be expected that

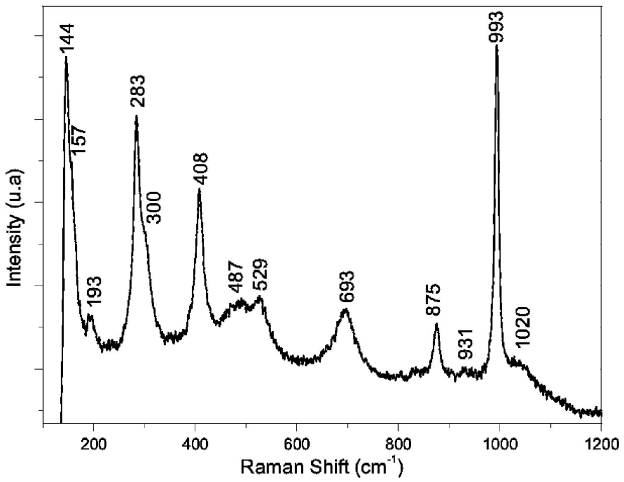

FIGURE 5. μ-Raman spectra of the $V_2O_5{\cdot}nH_2O$ film obtained for gelation time of 14 days.

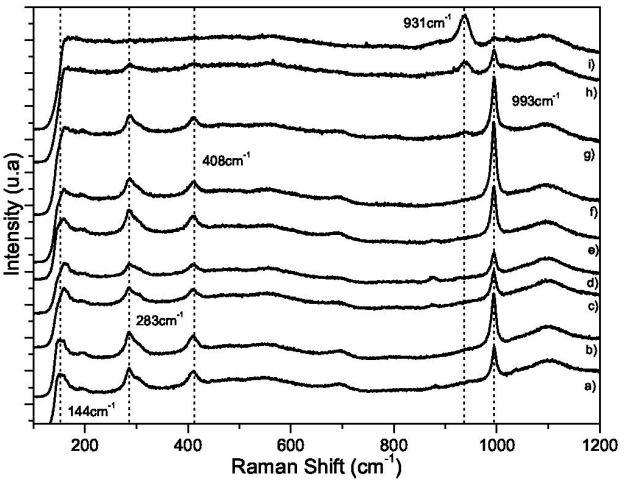

FIGURE 6. μ-Raman spectra of $V_2O_5{\cdot}nH_2O$ film at several temperatures: a) 20°C, b) 47°C, c) 97°C, d) 147°C, e) 204°C, f) 237°C, g) 272°C, h) 297°C and i) 330°C during 15 minutes for each isothermal.

while the water molecules leave the matrix material, the ionic component reduces its value by reducing the number of charge carriers increasing the electrical resistance for each of the cycles with the same way for activation energy (see Table VI). From the activation energies obtained, we can say that intermediate states exist between the conduction and valence band, which slightly depend on the water molecules present in the lattice and is in concordance with the reported for this type of films grown by other methods [9,11].

We observed a strong dependence between the energy for ionization of localized defects, with the number of measurement cycle. It is probably due to desorption of H_2O molecules (verified by X-ray diffraction results) which occupied oxygen vacancies, reducing the energy necessary for exciting thermally charged carriers doing more predominant the ionic contribution, as water molecules leave the material those vacancies are more and the contribution to electrical conductivity is due to polarons, increasing the activation energy. The crystallite sizes (001 and 003) with the thermal treatment, contribute to the increase of the activation energies too.

The hysteresis between consecutive cycles in the electrical properties, suggesting that water molecules leave the oxide matrix is irreversible for thermal treatment up to 250°C.

3.3. Raman spectroscopy analysis

Figure 5 shows the μ-Raman spectrum of $V_2O_5{\cdot}nH_2O$ film at room temperature. The records showed the normal vibrational modes of this material in 144 and 193 cm^{-1} corresponding to the lattice vibrations: 283, 408 and 993 cm^{-1}, assigned to the V=O vibrations modes, the first two as the bending and stretching of the third; 487 and 693 cm^{-1} for V-O-V of bending the first and stretching the second; 300 and 529 cm^{-1} agree with V_3-O bending and stretching respectively [12]. The bending vibrational lattice V-O-V-O-V... of long range located at 144 cm^{-1} shows a small band at 157 cm^{-1}, which is assigned by Cazzanelli *et al.*, [13] to lattice vibrations subjected to compressive deformations along the *a* direction.

Raman bands presents slight shifts on the positions reported for polycrystalline vanadium pentoxide, we believe this is mainly due to effects of the water molecules insertion on the matrix material. Additional to this, there are new bands at 875, 931 and 1020 cm^{-1}, which are frequently reported for V_2O_5 in amorphous phase [12,13] and correspond to V^{4+}=O and V^{5+}=O, for the last two respectively. The presence of these bands suggests the existence of both phases (crystalline-amorphous) due to deformation induced by water molecules within the oxide matrix. The correlation of the above results evidences four types of phases: $V_2O_5{\cdot}nH_2O$ crystalline with and without compressive deformation, amorphous structure (both detected by μ-Raman) and α-V_2O_5 (detected by XRD).

Figure 6 shows μ-Raman spectra of $V_2O_5{\cdot}nH_2O$ at different temperatures. Up to 47°C, the normal vibration modes of amorphous phase and the bending mode for V_2-O are inhibited, showing a high sensitivity to temperature and inferring a significant sensitivity of H_2O with pyramids that share one oxygen atom. The bending normal vibrational modes for the lattice disappear about 97°C, which are associated with changes in the wide-range correlation between the amount of basic units that composes the band according to Cazanelli *et al.* and are in agreement with disorder produce for thermal effects, while at this temperature the stressed lattice vibrations are predominant and the H_2O molecules introduced on these are strongly bonded. At about 272°C, the band corresponding to V^{4+}=O rises again, suggesting the presence of an amorphous phase. For 292°C, the band V^{5+}=O appears and V^{4+}=O increases its intensity, whereas for V-O-V stretching vibrations disappear after its amplitude is reduced significantly with temperature. Near 330°C, almost all the vibrational modes of vanadium pentoxide crystalline are inhibited, except those associated to lattice stressed bending, the stretching ones to V=O and V_3-O, implying that the in-

serted water molecules on the pyramids that share two oxygen atoms are practically null. At this temperature the vibrational modes of the amorphous phase prevail, inferring large structural disorder on the lattice due to the water desorption and the thermal effects that create vacancies on the oxide. The emergence of the amorphous phase for the high temperatures region, satisfactorily explains the increase in the electrical conductance due to the presence of a larger number of mixed valence vanadium ions, making it much more predominant the electronic conduction for this region than the ionic conduction by the aqueous phase leaving the film. When the material is taken back to room temperature, the vibrational modes are observed to correspond to crystalline V_2O_5, due to the reversibility in the process of H_2O desorption, which also allows the composite to maintain their crystalline structure to return to room temperature.

It is important to note from Fig. 6 that the variation of the main vibrational modes over temperature was less than 1%, inferring the presence of water molecules as a composite.

The Full Width at Half Maximum (FWHM) calculated by Gaussian settings as a function of temperature for the vibrational modes specific to the vanadyl oxygen (V=O), presents three points of relevant interest: for temperatures of 97 and 237°C, which are close to the reported values for which the level of gel hydration decreases to n=0.5 for T=120°C and n=0 for T=250°C [14], inferring possibly that the release of H_2O is stronger and irreversible for temperatures between 100 and 150°C, where crystallization of the new preferential direction becomes more evident. According to [15] changes in the FWHM, for the normal vibrations of V=O are associated with changes in the films crystalline quality.

4. Conclusions

The film growth $V_2O_5{\cdot}nH_2O$ for the sol-gel method, showed stability in the solvent amount (H_2O) with the gelation time (14 days), while thermal treatment evidenced the emergence of a new phase (α-V_2O_5), which seems to be energetically more stable with desorption of water. The degree of hydration of the gel composite decreases and is evident for (001), (003) peaks shift for XRD-diffractograms and this generated an increase in the activation energies for many consecutive cycles due to the oxide matrix H_2O leave, inducing a decrease of ionic component in the electrical conductivity. These results showed hysteresis in the thermal processes, suggesting that the water desorption is irreversible (between the room temperature and 250°C) and did not induce changes in the molecular order.

The desorption of water molecules by the film presents a reversible character between 250 and 330°C, presumably due to H_2O laminar adhered (and not linkage) over oxide matrix structure, characterized by a order-disorder transition. The films brought to that temperature do not crystallize in the *b* crystallographic direction, which is likely due to big disorders that the water molecules generate or by strong linkages between them in that particular direction.

Acknowledgments

This work was supported by Universidad Nacional de Colombia- Manizales.

1. Y.T. Oka Yao and N. Yamamoto, *Journal of Solid State Chemistry* **132** (1997) 323.
2. R. Subba *et al., Journal of Power Sources* **166** (2007) 244.
3. J. Livage, *Chemistry of Materials* **3** (1991) 578.
4. J. Livage, F Beteille, C. Roux, M. Chatry, and P. Davidson, *Acta Materialia* **46** (1998) 743.
5. B. Alonso and J. Livage, *Journal of Solid State Chemistry* **148** (1999) 16.
6. B.D. Cullity, *Elements of X-Ray Diffraction* (Addison-Wesley, Publishing Company, 1956)
7. P. Nam-Gyu, *et al., Journal of Power Sources* **103** (2002) 273.
8. Z.S. El Mandouh and M.S. Selim, *Thin Solid Films* **371** (2000) 259.
9. G.N. Barbosa, C.F.O. Graeff, and H.P. Oliveira, *Eclética Química* **30** (2005) 259.
10. S.H. Lee *et al., Solid State Ionics* **165** (2003) 111.
11. E. Cazzanelli, G. Mariotto, S. Passerini, and W.H. Smyrl, *Journal of Non-Crystalline Solids* **208** (1996) 89.
12. R.T. Rajendra Kumar *et al., Materials letters* **57** (2003) 3820.
13. C.J. Fontenot, *Investigation of the peroxovanadate sol-gel process and characterization of the gels* Ph.D. thesis. (Iowa State University, 2001)
14. C. Sanchez; M. Henry; J.C. Grenet and J. Livage, *Journal of Physics C-Solid State Physics* **15** (1982) 7133.
15. P. Balog, D. Orosel, Z. Cancarevic, S. Schounn and M. Jansen, *Journal of Alloys and Compounds* **429** (2007) 87.
16. M.S. Al-Assiri *et al., Optics and Laser Technology* **42** (2010) 994.